J. Fluid Mech. (1975), *vol.* 72, *part* 1, *pp.* 189–206
Printed in Great Britain

Turbulence measurements in smooth concentric annuli with small radius ratios

By K. REHME

Institut für Neutronenphysik und Reaktortechnik, Kernforschungszentrum, 75 Karlsruhe, Germany

(Received 12 September 1974 and in revised form 28 April 1975)

The structure of turbulence of fully-developed flow through three concentric annuli with small radius ratios was investigated experimentally for a Reynolds number range $Re = 2 \times 10^4$–2×10^5. Turbulence intensities were measured in three directions, and turbulent shear stresses in the radial and azimuthal direction, in annuli of radius ratios $\alpha = 0{\cdot}02$, $0{\cdot}04$ and $0{\cdot}1$, respectively. The results showed that the structure of turbulence for these asymmetric flows is not the same as that for symmetrical flows (tubes and parallel plates). The main difference between symmetrical and asymmetric flows is that, for the latter, the diffusion of turbulent energy plays an important role. This is the reason not only for the non-coincidence of the positions of zero shear stress and maximum velocity, but also for the failure of most turbulence models in calculating asymmetric flows.

1. Introduction

Our knowledge of the structure of turbulent flow through channels is based almost exclusively on experimental results concerning turbulent flow through tubes and between parallel plates. Such flows are very special cases of channel flows, because these channels generate a symmetrical velocity profile, and therefore the positions of zero shear stress and maximum velocity coincide. Flow channels of practical importance generally have more complex boundary conditions. In these non-circular channels, there are asymmetric velocity profiles; hence, the position of zero shear stress is not coincident with the position of maximum velocity. These asymmetric velocity profiles result from the interaction of two flow zones of different sizes and different kinetic energy of the turbulence field. It is to be expected that turbulent transport phenomena in such flows differ from those of symmetrical flows.

The simplest non-circular flow channel is a concentric annulus with smooth walls. The annulus also generates an asymmetric velocity profile, which is more asymmetric the smaller the radius ratio $\alpha = r_1/r_2$ of the inner and outer radii of the annulus. For this channel, a number of experimental investigations were performed on the pressure drop and the velocity distribution (table 1). Some significant deviations from the behaviour of symmetrical flows were shown, such as the non-coincidence of the position of zero shear stress with that of maximum

Author	Radius ratio α	Re range $\times 10^{-5}$	L/D_e	Quantities measured: $\overline{u}$	$\overline{(u'^2)}^{\frac{1}{2}}$	$\overline{(v'^2)}^{\frac{1}{2}}$	$\overline{(w'^2)}^{\frac{1}{2}}$	$\overline{u'v'}$
Brighton (1963)	0·0625	0·96–3·3	43·2	×	×	×	×	×
	0·125	0·89–3·1	46·3	×	×	×	×	×
	0·375	0·65–2·2	64·8	×	×	×	×	×
	0·562	0·46–1·5	92·6	×	×	×	×	×
Kjellström & Hedberg (1966)	0·446	1·5–3	54	×	×	×		×
Durst (1968)	0·446	1–10	54·8	×	×	×		×
Lawn & Elliott (1971)	0·088	0·62–2·3	52·7	×	×	×	×	×
	0·176	0·68–1·8	58·4	×	×	×	×	×
	0·396	0·68–1·5	79·6	×	×	×	×	×
This paper	0·0198	0·41–2·3	76·5	×	×	×	×	×
	0·0396	0·21–2·2	78·1	×	×	×	×	×
	0·0998	0·32–2·0	83·3	×	×	×	×	×

TABLE 1. Turbulence measurements in annuli

velocity, and a deviation from the law of the wall of the dimensionless velocity distribution in the inner zone of annuli with small radius ratios (Rehme 1974).

In contrast to the large number of experimental results on the flow in concentric annuli, only a few such are known, concerning the distribution of turbulence intensities and, hence, the kinetic energy of turbulence. The main parameters of the investigations reported in the literature are listed in table 1.

Brighton (1963) and Brighton & Jones (1964) for the first time published experimental results on turbulence intensities in three directions, and on radial shear stress; four different radius ratios were used by Brighton. Kjellström & Hedberg (1966) and Durst (1968) investigated turbulence in the same annulus experimentally; but they measured only the turbulence intensities in the axial and radial directions, besides the radial shear stress. Lawn & Elliott (1971) published results of turbulence measurements in annuli with three different radius ratios.

Both Brighton's and Lawn & Elliott's investigations covered fairly small radius ratios ($\alpha = 0{\cdot}0625$ and $\alpha = 0{\cdot}088$, respectively) with highly asymmetric velocity distributions, whereas Kjellström & Hedberg and Durst used a radius ratio of $\alpha = 0{\cdot}446$, for which the velocity distribution is only slightly asymmetric, and thus not relevant to asymmetric velocity distributions. But Brighton and Lawn & Elliott used spacers to fix the core tubes, which may strongly affect the velocity and turbulence distributions (Rehme 1974). Moreover, for the evaluation of his results, Brighton assumed that the positions of zero shear stress and of maximum velocity coincided, which has been proved to be untrue (Rehme 1974).

There are also some turbulence measurements on rod bundles, which are slightly relevant to the flow through annuli, because the inner zones of annuli are similar to the flow zones between the rods in rod bundles. Of course, this is true only of pitch-to-diameter ratios that are not too small, because secondary flows may occur owing to wall shear stress variations. Secondary flows are not possible in concentric annuli, for reasons of symmetry. Turbulence measurements in rod bundles are reported by Rowe (1973), Rowe, Johnson & Knudsen (1974) and Kjellström (1974).

From these measurements, no final conclusions can be drawn about the structure of turbulence in annuli, or hence about that in asymmetric flows. But it is important to have detailed knowledge of the structure of turbulence in asymmetric flows. This is necessary to decide whether there are major deviations from symmetrical flows. Generally it is concluded, from experimental results in non-circular channels, that the turbulence intensities, made dimensionless by the friction velocity, show a behaviour similar to that of those in tubes (Kjellström 1974). For the different methods of calculation by turbulence models, experimental results are also required to check whether the assumptions included in these models (which are generally based on knowledge of the flow in tubes and between parallel plates) are valid for asymmetric flows.

2. Apparatus

Experiments were performed using an open air rig, with annuli of three radius ratios ($\alpha = 0{\cdot}02$, $0{\cdot}04$ and $0{\cdot}1$), for a range of Reynolds numbers between 2×10^4 and 2×10^5.

The air rig and the outer brass tube (I.D. 99·97 mm, length 7500 mm) were those used earlier (Rehme 1972); and the turbulence measurements were run simultaneously with the investigations of pressure drop and velocity distributions reported by Rehme (1974). The cores consisted of a 9·98 mm diameter stainless-steel rod in the case of $\alpha = 0{\cdot}1$, and of 3·96 and 1·98 mm diameter aluminium wires in the cases $\alpha = 0{\cdot}04$ and $0{\cdot}02$, resulting in ratios of length to hydraulic diameter of 83·3, 78·1 and 76·5, respectively. The concentric position was achieved by using spacers at the inlet and outlet and, for $\alpha = 0{\cdot}1$, two other spacers. The wires were stretched and tensioned by a spring. In the annuli with $\alpha = 0{\cdot}04$ and $0{\cdot}02$, respectively, spacers were avoided, because measurements with the $\alpha = 0{\cdot}1$ annulus showed that the velocity and turbulence distributions were not fully established 27·8 hydraulic diameters downstream of the spacer, as outlined by Rehme (1974). The measurements were made at the open outlet of the test section. First, only the axial turbulence intensity $\overline{(u'^2)}^{\frac{1}{2}}$, radial intensity $\overline{(v'^2)}^{\frac{1}{2}}$ and the radial shear stress $\overline{u'v'}$ were investigated, with the radius ratios $\alpha = 0{\cdot}1$ and $\alpha = 0{\cdot}02$. For the radius ratio $\alpha = 0{\cdot}04$, the azimuthal intensity $\overline{(w'^2)}^{\frac{1}{2}}$ and the azimuthal shear stress $\overline{u'w'}$ (which must be zero because of symmetry) were investigated.

Next, the missing values for $\alpha = 0{\cdot}1$ and $\alpha = 0{\cdot}02$ ($\overline{(w'^2)}^{\frac{1}{2}}$, $\overline{u'w'}$) were recovered. Finally, the inner zone of the annulus with the radius ratio $\alpha = 0{\cdot}02$ was investigated, by means of a bent probe support. The first measurements covered only $\frac{1}{3}$ of this zone near the surface of zero shear stress; the bent probe support allowed measurements to be taken over 90 % of the flow zone.

Rehme (1972) described the apparatus (DISA hot-wire anemometer) for the turbulence measurements. The axial time-mean velocity was measured first by means of a Pitot tube (0·6 mm outer diameter) on a traverse in the radial direction. Hot-wire traverses were made with the wire normal to the flow, and with a slanting wire at yaw angles $\sim \pm 45°$. Finally, the Pitot tube traverse was repeated, to check whether the experimental conditions during all traverses had changed.

For evaluation of the hot-wire measurements, we adopted a method developed by Kjellström & Hedberg (1968, 1970), tested by Durst, Melling & Whitelaw (1971), and reviewed by Kjellström (1974). The hot-wire response was calibrated against the time-mean velocities measured by the Pitot tube. For that purpose, the exponent c in Collis's law (Collis & Williams 1959) was evaluated graphically. All results were computed on an IBM 360/165.

The relation

$$c = c_{\mathrm{av}} + K[(\rho\overline{u}) - (\rho\overline{u})_{\mathrm{av}}] \tag{1}$$

was proposed by Kjellström. 'av' denotes an average over the whole speed range of the calibration $K = -0{\cdot}0007782$, which takes into account the dependence of the exponent in Collis's law on the velocity. Equation (1) was not used for

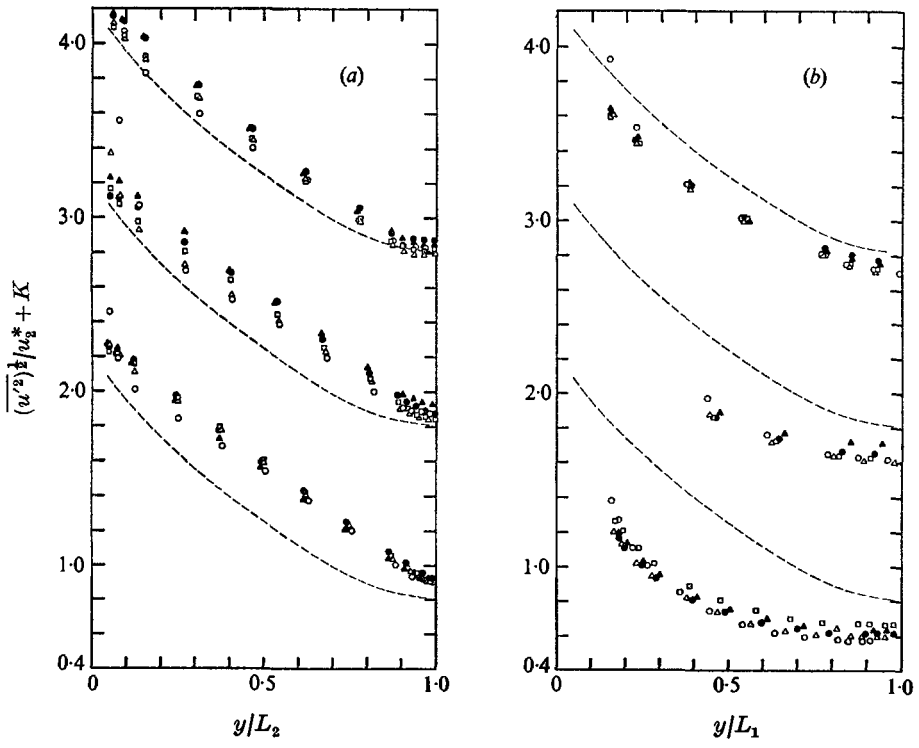

FIGURE 1. Experimental results for axial turbulence intensity against dimensionless distance from the wall: (*a*) outer zone; (*b*) inner zone. – – –, tube results of Laufer.

		$Re \times 10^{-4}$				
α	K	○	△	□	●	▲
0·02	0	4·155	8·067	11·36	16·04	23·36
0·04	1	2·063	3·981	7·036	10·47	21·57
0·1	2	3·248	7·498	8·964	16·61	20·22

computation of these results, however. Our results for this exponent showed a stronger dependence on velocity. Thus, for the calculations

$$c = c_{\mathrm{av}}[(\rho\bar{u})/(\rho\bar{u})_{\mathrm{av}}]^{0\cdot048} \tag{2}$$

was used, based on our measurements in the range $(\rho\bar{u}) = 6 - 50\,\mathrm{kg\,s^{-1}\,m^{-2}}$. The complete set of tabulated results may be acquired from Rehme (1975).

3. Results and discussion

3.1. *Turbulence intensities*

The turbulence intensities measured in this investigation are plotted in figures 1–3, for three directions, against dimensionless distance normal to the wall. The figures each show the turbulence intensities of the outer zone on the left side (*a*), and of the inner zone on the right side (*b*), for five Reynolds numbers and the three diameter ratios. The turbulence intensities measured are made dimensionless by the friction velocities of the respective walls.

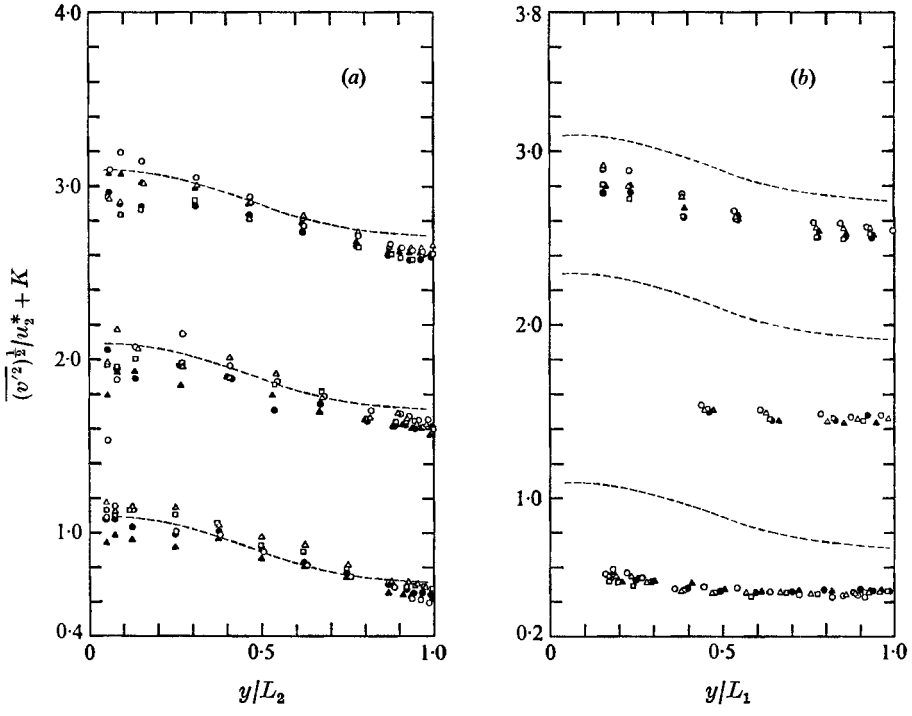

FIGURE 2. Experimental results for radial turbulence intensity against dimensionless distance from the wall: (*a*) outer zone; (*b*) inner zone. Symbols as in figure 1.

The friction velocities hang on the values of the wall shear stresses, which were deduced from a force balance (on the basis of the friction factors measured), and on the position of zero shear stress measured by the hot wire. One piece of evidence for accurate determination of the zero-shear position is the reasonable agreement of the shear stress distributions measured by the hot wire with those calculated from a force balance. Another piece of evidence is the excellent agreement of the zero-shear positions measured by the hot wire with those calculated by the experimental wall shear stresses at the inner and outer surfaces measured by Preston tubes. Wall shear stress measurements by Preston tubes require the validity of universal laws of the velocity distribution in the y^+ range covered by the Preston tubes, a condition which is critical especially for the inner zones. The experimental velocity profiles showed that this assumption was sufficiently well satisfied for these measurements. The Preston tube covered the range of the four lowest y^+ of the experimental velocity profiles (Rehme 1974, figure 10). Thus the friction velocities were calculated on the basis of the equations reported by Rehme (1974, (7)–(9) and (12)–(14)). For comparison, the turbulence intensities measured in tubes by Laufer (1954) are included in the diagrams as dashed lines.

The turbulence intensities in the axial direction are higher than those in tubes, as measured by Laufer in the outer zone of the three annuli; and they are higher, the lower the radius ratio. The dependence of the axial intensity in the outer zone on distance from the wall is also different from tubes, because this is nearly

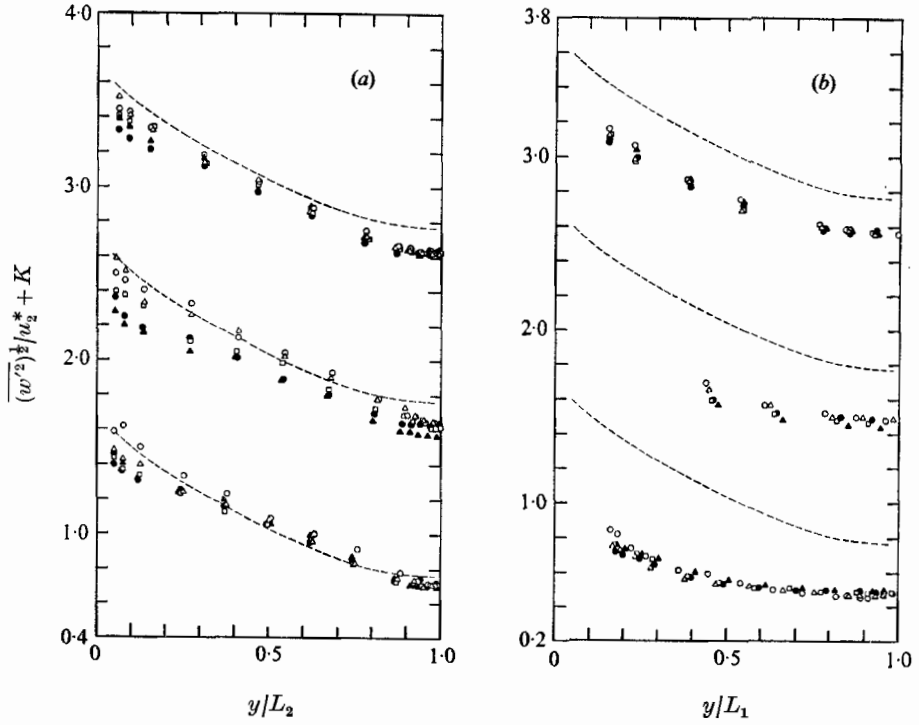

FIGURE 3. Experimental results for azimuthal turbulence intensity against dimensionless distance from the wall: (*a*) outer zone; (*b*) inner zone. Symbols as in figure 1.

linear over a wide range ($0{\cdot}1 < y/L_2 < 0{\cdot}8$). The values in the inner zone are significantly lower than the tube values of Laufer. The distance between the tube values and the values in the inner zone of annuli increases with decreasing radius ratios. For $\alpha = 0{\cdot}1$, the dependence of inner-zone intensities on distance from the wall is similar to that of tubes. For the two smaller radius ratios, the axial intensity in the inner zone is nearly constant over a larger part of the flow zone, and increases only close to the wall. Influence of Reynolds number on dimensionless turbulence intensities cannot be detected unequivocally. Turbulence intensities in the radial and azimuthal directions generally show the same behaviour as the tube values. In the outer zone, the annulus values are nearly parallel to the tube values: they increase slightly with decreasing radius ratio. On the other hand, the intensities in the inner zone differ greatly from the tube values: the annulus results are increasingly lower than Laufer's values for tubes with decreasing radius ratio. Collapse of intensity measurements of the inner and outer zones is also not achieved by dividing intensities by local shear stress, instead of wall shear stress.

Turbulence intensities in all directions have their minimum values in the region of the zero shear stress position. This observation does not coincide with the results of Hanjalić & Launder (1968) on a parallel-plate channel with non-identical roughnesses at the walls. An asymmetrical velocity distribution occurs also in this case. The measurements by Hanjalić & Launder showed a minimum

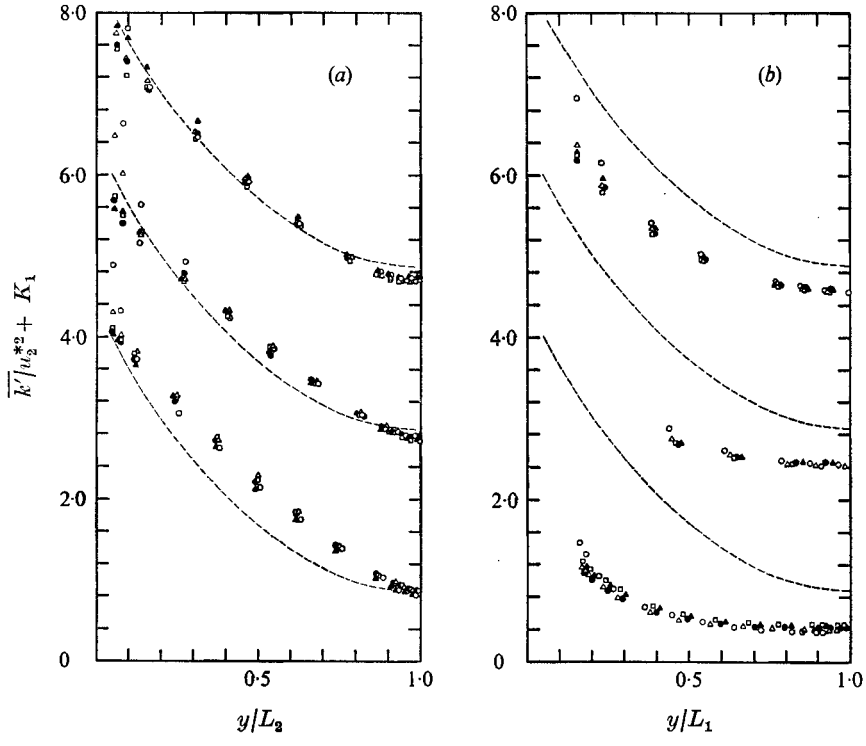

FIGURE 4. Experimental results for kinetic energy of turbulence against dimensionless distance from the wall: (*a*) outer zone; (*b*) inner zone. $\alpha = 0{\cdot}02$ ($K_1 = 0$); $\alpha = 0{\cdot}04$ ($K_1 = 2$); $\alpha = 0{\cdot}1$ ($K_1 = 4$). Other symbols as in figure 1.

value of axial and radial turbulence intensities at roughly 80 % of the profile length of the smaller flow zone, whereas the azimuthal intensity showed a minimum at the zero shear stress position.

In summary, we may state that measurements of turbulence intensities of the flow through annuli show that the structure of turbulence is highly non-isotropic in the outer flow zone, whereas this is less marked in the inner zone, if the regions $y/L > 0{\cdot}5$ are considered.

3.2. *Kinetic energy of turbulence*

The kinetic energy of turbulence, defined as

$$\overline{k'} = 0{\cdot}5(\overline{u'^2} + \overline{v'^2} + \overline{w'^2}), \tag{3}$$

can be calculated as the sum of the intensities in the three directions. Figure 4 shows the calculated values divided by the square of the respective friction velocities. For comparison, the curves representing Laufer's tube results are once more included in the diagrams. Apart from small zones near the wall and near the zero-shear position, the experimental results for annuli in the outer zone are higher than the tube values. The dependence of the data on the distance from the wall is nearly linear in a range $0{\cdot}2 < y/L_2 < 0{\cdot}7$ for the radius ratios $\alpha = 0{\cdot}04$

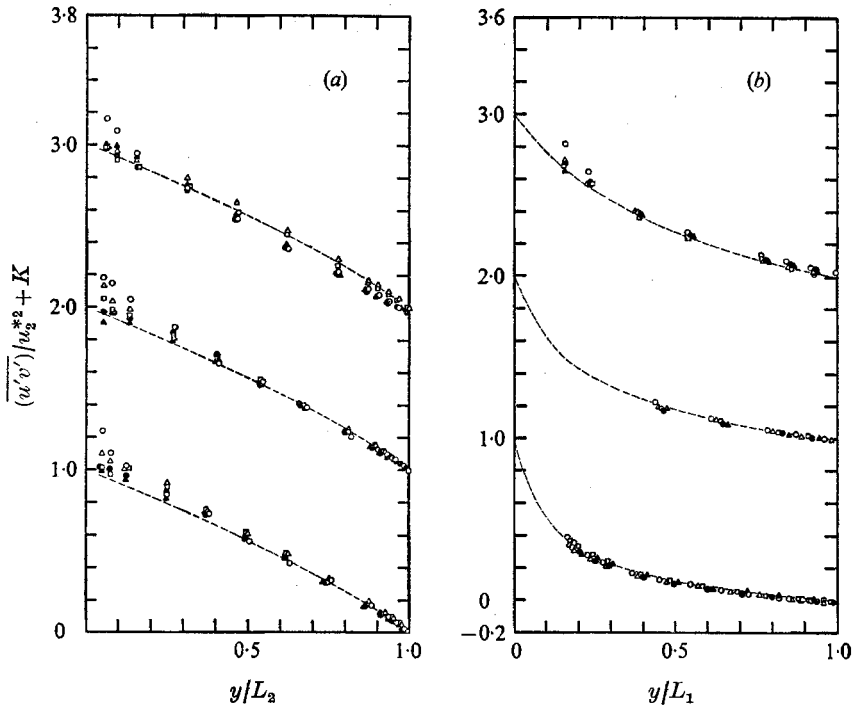

FIGURE 5. Experimental values of radial shear stress against dimensionless distance from the wall: (*a*) outer zone; (*b*) inner zone. Symbols as in figure 1. – – –, calculated.

and 0·02. In the inner zone, again kinetic energy is much less than in tubes. Moreover, the results show that the minimum of the kinetic energy of turbulence coincides with the position of zero shear stress. This is important, because the physical phenomena causing the non-coincidence of the position of zero shear stress with that of maximum velocity can thus be explained reasonably.

3.3. *Shear stress and correlation coefficient*

Figure 5 shows the measured distribution of the radial shear stress. For comparison, the profiles calculated from the pressure drop and the position of zero shear stress measured at $Re = 10^5$ are included as dotted lines. A balance of forces yields

$$\tau P = \frac{\Delta p}{\Delta L} A, \tag{4}$$

with the wetted perimeter P, the pressure drop Δp along the length ΔL, and the flow cross-section A. Assuming $\partial p/\partial r = 0$ for fully-developed flow through annuli, we get, for the inner zone,

$$\frac{\tau}{\tau_{w_1}} = \frac{\beta^2 - (r/r_2)^2}{\beta^2 - \alpha^2} \frac{\alpha}{(r/r_2)}; \tag{5}$$

and, for the outer zone,

$$\frac{\tau}{\tau_{w_2}} = \frac{(r/r_2)^2 - \beta^2}{1 - \beta^2} \frac{1}{(r/r_2)}. \tag{6}$$

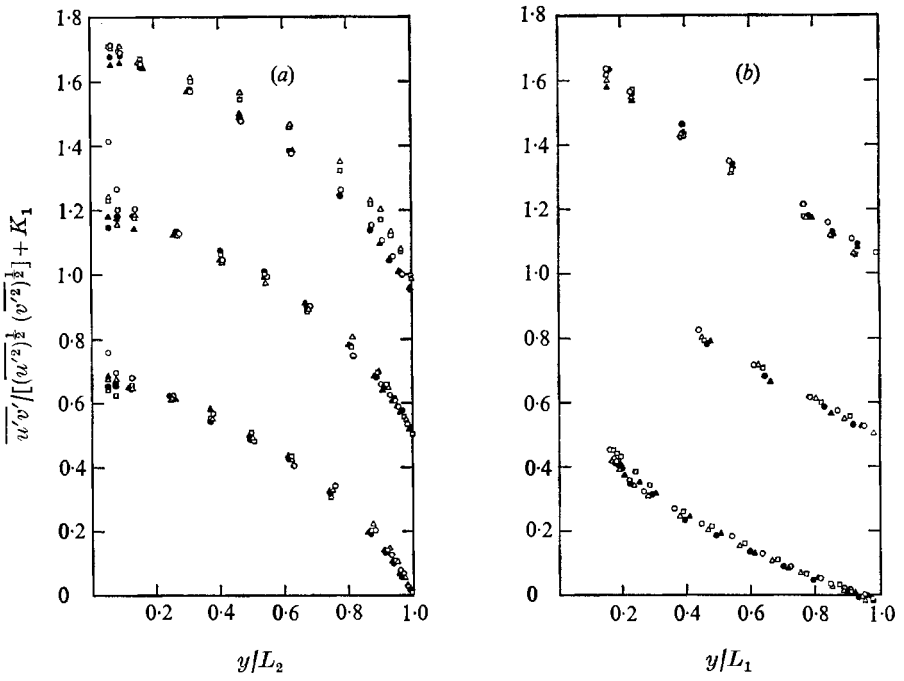

FIGURE 6. Experimental results for correlation coefficients *vs.* dimensionless distance from the wall: (*a*) outer zone; (*b*) inner zone. $\alpha = 0{\cdot}02$ ($K_1 = 0$); $\alpha = 0{\cdot}04$ ($K_1 = 0{\cdot}5$); $\alpha = 0{\cdot}1$ ($K_1 = 1{\cdot}0$). Other symbols as in figure 1.

($\beta = r_0/r_2$ is the dimensionless position of zero shear stress.) There is only slight influence of Reynolds number on the calculated shear stress profile: it was neglected here.

The calculated and the measured profiles in the outer zone are in good agreement; agreement is excellent in the region $0{\cdot}5 < y/L_2 < 1{\cdot}0$. Near the wall, there are small deviations especially for low Reynolds numbers, the measured values being higher than the calculated. The reason for this is supposed to lie in heat conduction effects from hot wires close to the wall. For the inner zone, agreement between measurements and calculation is excellent for the diameter ratios $\alpha = 0{\cdot}04$ and $0{\cdot}02$. The results for $\alpha = 0{\cdot}1$ suggest that a slightly higher inner wall shear stress ought to have been measured; but such results are not very conclusive, since spacers were used in this case, which disturbed the flow, as Rehme (1974) explained.

Figure 6 shows the measured correlation coefficients in the inner and outer zones, respectively. The correlation coefficient $\overline{u'v'}/((\overline{u'^2})^{\frac{1}{2}}(\overline{v'^2})^{\frac{1}{2}})$ in the outer zone is higher than in the inner zone, which also holds near the wall. This result is in contrast to the measurements of Durst (1968), who used a radius ratio of $\alpha = 0{\cdot}446$ however. A difference between the results of Durst and the new measured values is also that there is no similarity of the profiles near the position of zero shear stress.

The gradient of the correlation coefficient in the case of the small radius ratios used here is steeper in the outer zone, and the curvature of the profiles in the

inner and outer zones is different. Durst's results with the annulus showed, too, that there was a region near the walls where the correlation coefficient was nearly independent of distance from the walls, which is also the case in tube flow.

The results for annuli with small radius ratios do not exhibit such behaviour. On the contrary, in the outer zone the correlation coefficient slightly increases towards the wall, whereas we find a strong increase in the correlation coefficient near the wall in the inner zone, which is of course due to the corresponding trend of the shear stress. Compared with tube results, the correlation coefficient at best shows a similar trend near the position of zero shear stress in the outer zone; otherwise, the trend is quite different.

3.4. *Eddy viscosities*

The eddy viscosities ϵ_r^u in the radial direction can be calculated easily, using measured velocity distributions (Rehme 1974) and shear stress distributions computed from (5) and (6), based on wall shear stresses calculated from the measured position of zero shear stress. In a dimensionless form, we get

$$\frac{\epsilon_r^u}{Lu^*} = \frac{\tau}{\tau_w}\left[\frac{\partial(u/u_m)}{\partial(y/L)}\right]^{-1}\frac{u^*}{u_m}. \tag{7}$$

The calculated eddy viscosities are plotted in figure 7 for the $\alpha = 0{\cdot}02$ annulus. The results for the other two annuli do not differ significantly: they are therefore omitted from this paper. For comparison, two relationships well known in the literature are included, the curve representing tube measurements of Nikuradse (1932) and the equation developed by Reichardt (1951):

$$\frac{\epsilon_r^u}{Lu^*} = \frac{\kappa}{3}\left(0{\cdot}5 + \left(\frac{z}{r}\right)^2\right)\left(1 - \left(\frac{z}{r}\right)^2\right), \tag{8}$$

with $\kappa = 0{\cdot}4$ and $z/r = 1 - y/L$.

The experimental values in the outer zone are described well by the two curves. For $y/L_2 > 0{\cdot}8$, the data are very scattered, because the velocity gradient in this region becomes very small, resulting in large uncertainties. For $y/L_2 \to 1$, the velocity gradient and the shear stress have opposite signs, because the positions of zero shear stress and maximum velocity do not coincide. In this region, application of an eddy viscosity is not meaningful; but the region is very small, and not very important for calculations of turbulent flow through annuli; thus it may be neglected. It should be noted that an adequate description of the mean velocity distribution can be obtained by eddy diffusivity models, whereas the wall shear stresses, especially at the inner wall, are not calculated correctly. In the inner zone, a discrepancy is observed between the predicted and the measured eddy viscosities. In the wall region, the measured eddy viscosities are below the two curves of Nikuradse and Reichardt. In the middle of the flow region, the maximum value of the eddy viscosity seems to be higher than in tubes, and obviously occurs at a higher y/L_2. In spite of the greater scatter, a tendency of the measurements towards zero may be detected in the region close to the zero-shear position unlike the results in the outer zone. Measurements of the eddy viscosity by Jonsson & Sparrow (1966), using three radius ratios (0·28, 0·56 and 0·75) higher

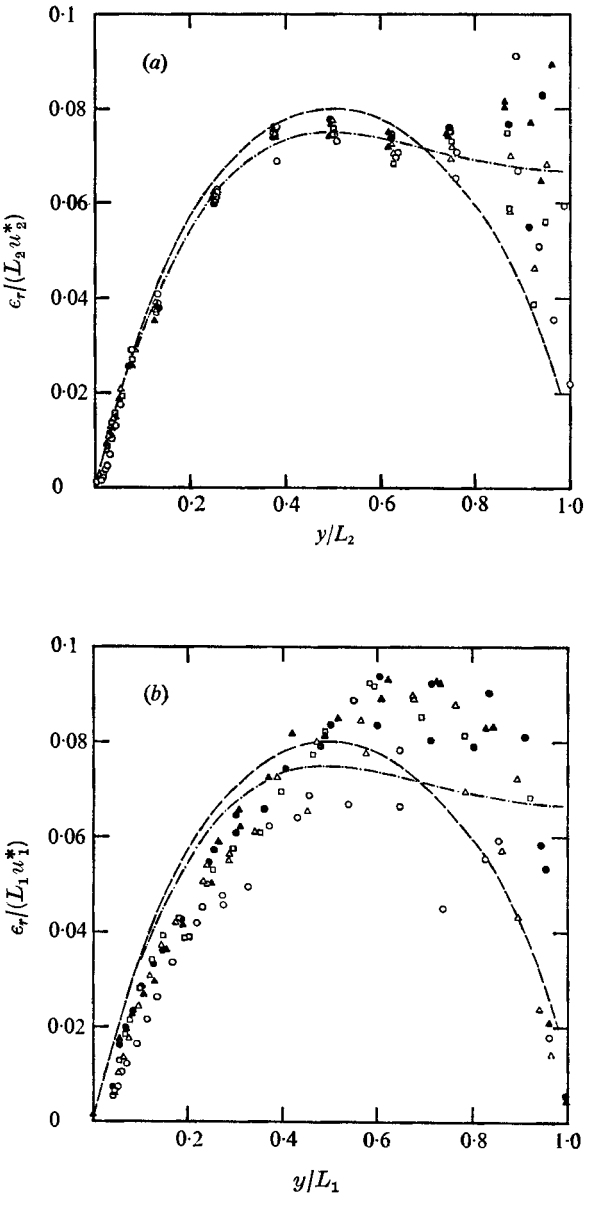

FIGURE 7. Experimental results for radial eddy viscosity: (*a*) outer zone; (*b*) inner zone. $\alpha = 0{\cdot}02$. Tube results: – – –, Nikuradse; – · –, Reichardt.

	○	△	□	●	▲
$Re \times 10^{-4}$	4·05	7·89	11·70	15·76	20·93

than in this study and thus for weakly asymmetric flows, showed no differences between inner and outer zones. All their results for different Reynolds numbers, radius ratios and flow zones coincide within the experimental scatter. Jonsson & Sparrow concluded from their measurements that the eddy viscosities are

independent of the geometry of the channel wall in the range of diameter ratios investigated. The new results show that, for strongly asymmetric flows, eddy viscosities are affected by channel geometry.

3.5. *Comparison with results from the literature*

Of data in the literature, only those from Brighton (1963) and Lawn & Elliott (1971) are suitable for comparison with the presents results, because only in these experiments were intensities measured in all directions. Such comparison is now made, with intensities related to the respective friction velocities. In order to provide a basis for comparison, friction velocities are calculated with the experimentally determined position of zero shear stress (Rehme 1974); thus the position of zero shear stress is calculated with the relation

$$\frac{\beta-\alpha}{1-\beta} = \alpha^{0.386} \tag{9}$$

for the investigations of Brighton and Lawn & Elliott.

Brighton's results could be re-calculated directly, because they were tabulated. Those of Lawn & Elliott were given only in diagrams: turbulence intensities for three values of the dimensionless profile length (namely, $y/L = 0{\cdot}2$, $0{\cdot}5$ and $0{\cdot}8$), for both the inner and outer zones, were taken from these. To evaluate the dependence of turbulence intensities on radius ratio of the annulus, all results were related to the tube values of Laufer. The latter were taken as a standard, because they are well known in the literature, although the shape of the profiles of the turbulence intensities in the present study is in better agreement with the results on a plate channel obtained by Comte-Bellot (1965). For the three values of dimensionless profile length, turbulence intensities normalized to Laufer's results were taken from the diagrams for all Reynolds numbers investigated. Afterwards, the values were averaged with respect to the Reynolds numbers, and finally also with respect to dimensionless profile length.

Figure 8 shows the results, some of which are very scattered. Nevertheless, general trends of variation of turbulence intensities and kinetic energy of turbulence with the radius ratio can be observed. A slight decrease of the intensities and the turbulent energy with increasing radius ratios occurs in the outer zone of annuli.

The axial turbulence intensity for a radius ratio approaching zero is about 20% higher than in the results of Laufer. A radius ratio $\alpha = 0$ is the limiting value for a tube. An explanation of the relatively high values may be found in the fact that Laufer's results are on the low side. Measurements in tubes by Kjellström & Hedberg (1966), by Coantic (1962) and by Rehme (1972) yield values higher than Laufer's (cf. Durst 1968). Also, results of Comte-Bellot (1965) in parallel-plate flow yield values of the axial turbulence intensity about 15–20 % higher than Laufer's. In the case of radial and azimuthal intensities, the limiting case $\alpha \to 0$ shows a value of nearly 1. This seems to be reasonable, because Laufer's radial and azimuthal intensities are in good agreement with results of other authors. In the inner zone of annuli, we find strongly decreasing turbulence intensities and

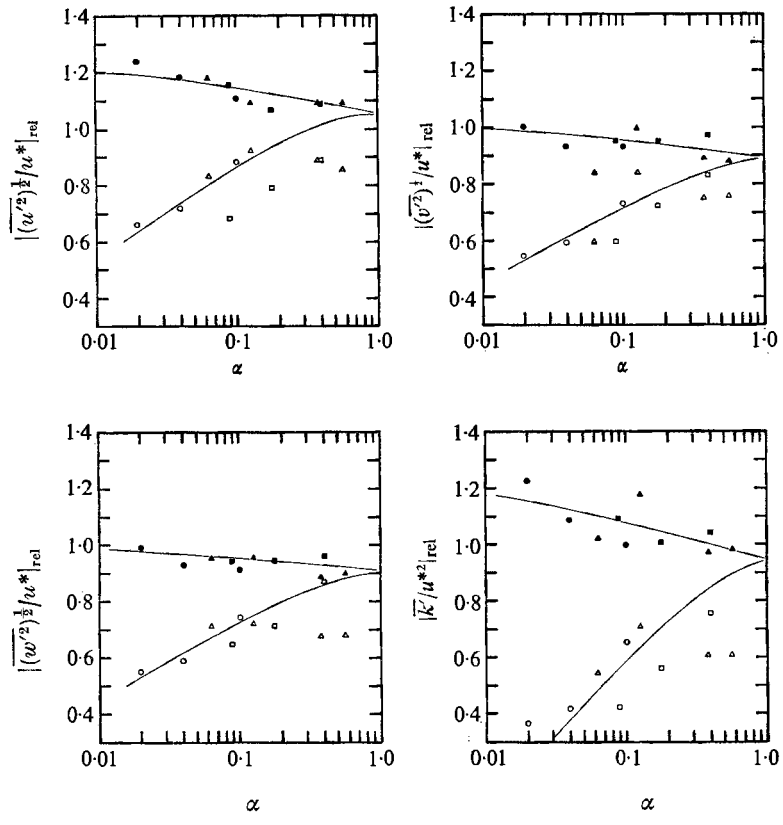

FIGURE 8. Relative turbulence intensity and kinetic energy of turbulence against radius ratio for the inner (open symbols) and outer zone (solid symbols). △, ▲, Brighton; □, ■, Lawn & Elliott; ○, ●, present results

decreasing kinetic energy of turbulence with decreasing radius ratio. These tendencies are in agreement with those found in rod-bundle results by Kjellström (1974) and Rowe (1973).

Figure 9 compares one characteristic example of the new results ($\alpha = 0{\cdot}02$, $Re = 2{\cdot}336 \times 10^5$) with the predictions of turbulence intensities in different channels by Bobkov, Ibragimov & Sabelev (1968). These authors generalized experimental results on turbulence intensities from different investigations, through the empirical formula

$$\overline{(u_i'^2)^{\frac{1}{2}}}/U_* = A \exp[-B(y/L)], \tag{10}$$

with

$$U_* = \overline{u}(1 - \overline{u}_m/\overline{u}_{\max}). \tag{11}$$

($\overline{u}$ is the local time-mean velocity, $\overline{u}_m$ the average across the channel, and $\overline{u}_{\max}$ the maximum value of the channel. A and B are constants different for the different directions.)

The comparison demonstrates that the experimental results for axial turbulence intensity in the outer zone are predicted rather well. The shape of the radial and azimuthal intensity in the outer zone is described quite well by the predictions,

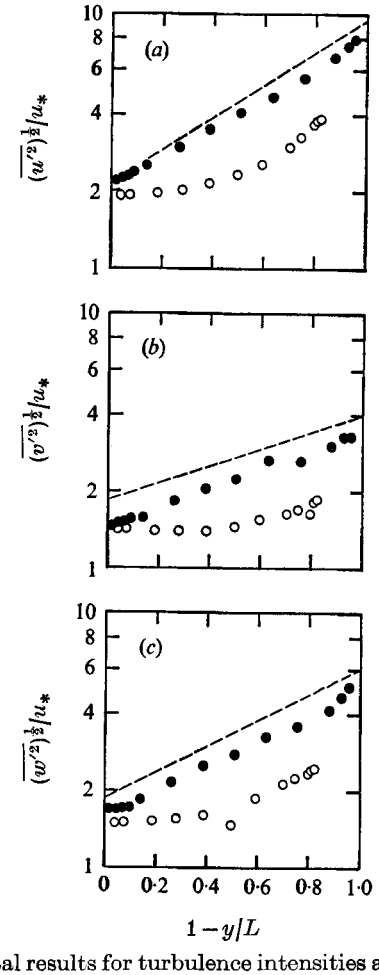

FIGURE 9. Experimental results for turbulence intensities and predictions by Bobkov *et al.*, $Re = 2{\cdot}336 \times 10^5$. $\alpha = 0{\cdot}02$. Inner zone, open symbols; outer zone, solid symbols. (*a*) Axial intensity, (*b*) radial intensity, (*c*) azimuthal intensity.

too, although the measurements are 20–25 % below the predicted curves. On the other hand, the prediction completely fails for the inner zone of the annulus, in terms of both absolute values and the general trend across the flow zone. Thus it must be concluded that the prediction of turbulence intensities by the method of Bobkov *et al.* is not adequate for asymmetric flows.

3.6. *Comparison with predictions by Hanjalić*

Hanjalić (1970) developed a model of turbulence, wherein transport equations are solved for the shear stress, the kinetic energy of turbulence and the energy dissipation rate. Together with the mean momentum equation, this model is a simpler version for two-dimensional boundary-layer flows of the more general one suggested by Hanjalić, using seven transport equations. It is obviously most adequate for asymmetric flows, since it does not rely on the assumption of a mixing length. Hanjalić (1970) tested his model against different asymmetric flows,

including flow through a smooth annulus with a small radius ratio. (See also Hanjalić & Launder 1972.) For that purpose, Hanjalić compared the predictions by his model with the results of Lawn & Elliott (1971) on an annulus with a radius ratio $\alpha = 0{\cdot}088$. The predicted profiles of mean velocity and shear stress agree well with the experimental data. The calculated positions of zero shear stress and maximum velocity do not coincide. The position of zero shear stress predicted by Hanjalić lies slightly nearer to the inner surface than the experimental result of Lawn & Elliott. The results of this investigation (Rehme 1974) also show a tendency for the zero shear position to be nearer the inner surface than it is according to the experimental values of Lawn & Elliott.

On the other hand, the predicted position of maximum velocity lies slightly nearer to the outer surface than the position as measured by Lawn & Elliott, whereas the new results tend to the opposite direction. Comparing predictions as to the position of maximum velocity by the model of Hanjalić with the equation of Kays & Leung (1963) for the same also shows that the former are probably too high.

These differences may be caused by a 'small departure from the usual practice' (Hanjalić 1970) in the calculation of flow through smooth concentric annuli. Since turbulence models are valid only at high Reynolds numbers, the viscous sublayer is neglected, and the boundary condition at the grid point nearest to the wall was chosen so as to meet the universal logarithmic velocity profile at this point. Hanjalić generally applied the form of this profile suggested by Patel (1965):

$$u^+ = 5{\cdot}5 \log_{10} y^+ + 5{\cdot}45. \tag{12}$$

But, for calculation of flow through annuli, Hanjalić changed the additive constant 5·45 in (12), near the inner core-surface, to

$$B = 5{\cdot}45\,(r_1/r_2)^{0{\cdot}1}. \tag{13}$$

This was to account for influence of large curvature, since the data of Lawn & Elliott and others showed that the velocity at the edge of the sublayer falls below the universal logarithmic velocity profile. The results of the present investigation, even for larger curvature at the inner surface, do not exhibit differences from the logarithmic velocity profile near the wall, especially for high Reynolds numbers. Thus, it may be suspected that, in predicting profiles, Hanjalić accommodated the data of Lawn & Elliott by varying the constant B according to (13). Moreover, it is interesting to note that the predictions of the positions of zero shear stress and maximum velocity by Hanjalić's model do not show an appreciable influence of Reynolds number, whereas the present results show such influence slightly for a radius ratio $\alpha = 0{\cdot}1$ (with spacers), the more so at lower radius ratios.

4. Conclusions

This experimental study of the flow and turbulence distribution in annuli with small radius ratios showed general differences between symmetrical (tube) and strongly asymmetric flows. Knowledge of symmetrical flows cannot, therefore, be extended uncritically to asymmetric ones. In particular, this study indicated that the turbulence intensity profiles are not universal, if they are made dimensionless by friction velocity. Turbulence intensities and kinetic energy of turbulence are significantly lower in the inner zone of annuli than in the outer. Differences between the inner and the outer zones increase with decreasing radius ratios, or with increasing asymmetry.

Based on results reported in the literature, and on new measurements, this study estimated the dependence of turbulence intensities on the radius ratio of concentric annuli.

For adequate calculation of asymmetric flows, it is necessary to use complex turbulence models, such as that proposed by Hanjalić (1970) and Hanjalić & Launder (1972), which is probably the most adequate, of practical importance, available at present. This study provided experimental results, always necessary to test such advanced models.

The author wishes to express his gratitude to Mr E. Mensinger and Mr G. Wörner for their invaluable help with the construction of the test rig, performance of the experiments and evaluation of the results. This paper is a portion of the author's thesis (Rehme 1975) approved of the Faculty of Mechanical Engineering, University of Karlsruhe, in partial fulfilment of the requirements for the *venia legendi* in Thermo- and fluid dynamics.

REFERENCES

BOBKOV, V. P., IBRAGIMOV, M. KH. & SABELEV, G. I. 1968 Generalization of experimental results for the turbulence intensity in turbulent flow in ducts of various cross-sections. *IZV. AN SSSR, Mekh. zhi. i Gaza* **3**, 162. (See also *Kernforschungszentrum Karlsruhe Rep.* KFK-tr-361.)

BRIGHTON, J. A. 1963 The structure of fully-developed turbulent flow in annuli. Ph.D. thesis, Purdue University.

BRIGHTON, J. A. & JONES, J. B. 1964 Fully-developed turbulent flow in annuli. *J. Basic Engng*, D **86**, 835.

COANTIC, M. 1962 Contribution à l'étude théorique et experimentale de l'écoulement turbulent dans un tube circulaire. *Publ. Sci. Tech. Ministère d l'Air, Paris, Note Tech.* no. 113.

COLLIS, D. C. & WILLIAMS, M. J. 1959 Two-dimensional convection from heated wires at low Reynolds numbers. *J. Fluid Mech.* **6**, 357.

COMTE-BELLOT, G. 1965 Écoulement turbulent entre deux parois parallèles. *Publ. Sci. Tech. Ministére d l'Air, Paris*, no. 419.

DURST, F. 1968 On turbulent flow through annular passages with smooth and rough cores. M.Sc. thesis, Imperial College, London.

DURST, F., MELLING, A. & WHITELAW, J. H. 1971 The interpretation of hot wire signals in low turbulence flows. *Imperial College, London, Rep.* ET/TN/B/5.

HANJALIĆ, K. 1970 Two-dimensional asymmetric flow in ducts. Ph.D. thesis, University of London.

HANJALIĆ, K. & LAUNDER, B. E. 1968 Fully-developed flow in rectangular ducts of non-uniform surface texture. I. An experimental investigation. *Imperial College, London, Rep.* TWF/TN/48.

HANJALIĆ, K. & LAUNDER, B. E. 1972 A Reynolds stress model of turbulence and its application to thin shear flows. *J. Fluid Mech.* **52**, 609.

JONSSON, V. K. & SPARROW, E. M. 1966 Turbulent diffusivity for momentum transfer in concentric annuli. *J. Basic Engng*, **88**, 550.

KAYS, W. M. & LEUNG, E. Y. 1963 Heat transfer in annular passages: hydrodynamically developed turbulent flow with arbitrarily prescribed heat flux. *Int. J. Heat Mass Transfer*, **6**, 537.

KJELLSTRÖM, B. 1974 Studies of turbulent flow parallel to a rod bundle of triangular array. *AB Atomenergi, Studsvik, Rep.* AE-487.

KJELLSTRÖM, B. & HEDBERG, S. 1966 On shear stress distributions for flow in smooth or partially rough annuli. *AB Atomenergi, Studsvik, Rep.* AE-243.

KJELLSTRÖM, B. & HEDBERG, S. 1968 Calibration experiments with a DISA hot-wire anemometer. *AB Atomenergi, Studsvik, Rep.* AE-338.

KJELLSTRÖM, B. & HEDBERG, S. 1970 Die Eichung eines DISA Hitzdrahtanemometers und Bestätigung der Eichung durch Messungen in einem zylindrischen Kanal. *DISA Inf.* **9**, 8.

LAUFER, J. 1954 The structure of turbulence in fully-developed pipe flow. *N.A.C.A. Tech. Note*, no. 1174.

LAWN, C. J. & ELLIOTT, C. J. 1971 Fully-developed turbulent flow through concentric annuli. *C.E.G.B. Rep.* RD/B/N/1878.

NIKURADSE, J. 1932 Gesetzmäßigkeiten der turbulenten Strömung in glatten Rohren. *VDI-Fosch. Heft*, no. 356.

PATEL, V. C. 1965 Calibration of the Preston tube and limitations on its use in pressure gradients. *J. Fluid Mech.* **23**, 185.

REHME, K. 1972 Untersuchungen der Turbulenz- und Schubspannungsverteilung an einem Kreisrohr mit einem Hitzdraht-Anemometer. *Kernforschungszentrum Karlsruhe Rep.* KFK-1642.

REHME, K. 1974 Turbulent flow in smooth concentric annuli with small radius ratios. *J. Fluid Mech.* **64**, 263.

REHME, K. 1975 Turbulente Strömung in konzentrischen Ringspalten. *Kernforschungszentrum Karlsruhe Rep.* KFK-2099.

REICHARDT, H. 1951 Vollständige Darstellung der turbulenten Geschwindigkeitsverteilung in glatten Leitungen. *Z. angew. Math. Mech.* **31**, 208.

ROWE, D. S. 1973 Measurement of turbulent velocity, intensity and scale in rod bundle flow channels, *Battelle Northwest Labs. Rep.* BNWL-1736.

ROWE, D. S., JOHNSON, B. M. & KNUDSEN, J. G. 1974 Implications concerning rod bundle crossflow mixing based on measurement of turbulent flow structure. *Int. J. Heat Mass Transfer*, **17**, 407.